Electronic Supplementary Material (ESI) for Physical Chemistry Chemical Physics.

Supporting Information for

Comprehensive Understanding of the Intrinsic Mobility in III-VI Monolayers

Jianhui Chen[1], Xiaolin Tan[1], Peng Lin[1], Baisheng Sa[1,*], Jian Zhou[2], Yinggan Zhang[3], Cuilian Wen[1] and Zhimei Sun[2,**]

[1]*Key Laboratory of Eco-materials Advanced Technology, College of Materials Science and Engineering, Fuzhou University, Fuzhou 350108, P. R. China*

[2]*School of Materials Science and Engineering, and Center for Integrated Computational Materials Science, International Research Institute for Multidisciplinary Science, Beihang University, Beijing 100191, P. R. China*

[3]*College of Materials, Xiamen University, Xiamen 361005, P. R.China*

*To whom the correspondence should be addressed: bssa@fzu.edu.cn.

**To whom the correspondence should be addressed: zmsun@buaa.edu.cn.

Table S1. Phonon dispersion frequencies (in unit of meV) at the high symmetry points of 1BZ for MX monolayers

System	Phonon modes	Γ	K	M
InS	ZA	0	5.12	5.05
	TA	0	6.78	7.32
	LA	0	8.29	10.76
InSe	ZA	0	4.38	4.31
	TA	0	5.02	6.95
	LA	0	7.29	8.10
InTe	ZA	0	4.61	4.71
	TA	0	4.72	4.92
	LA	0	5.35	7.66
GaS	ZA	0	9.01	8.64
	TA	0	9.44	8.88
	LA	0	11.20	15.27
GaSe	ZA	0	7.97	7.69
	TA	0	7.99	7.80
	LA	0	8.89	12.49
GaTe	ZA	0	4.80	4.71
	TA	0	5.39	5.54
	LA	0	5.88	8.99

Table S2. The individual phonon resolved electron mobility ($cm^2 \cdot v^{-1} \cdot s^{-1}$) of all modes at 300 K in MX monolayers

Modes	InS	InSe	InTe	GaS	GaSe	GaTe
ZA	6.11×10^{4}	5.79×10^{5}	5.40×10^{5}	4.14×10^{5}	1.60×10^{5}	1.19×10^{8}
TA	3.24×10^{7}	5.27×10^{7}	3.74×10^{5}	5.81×10^{6}	6.18×10^{5}	2.59×10^{6}
LA	4.76×10^{4}	2.36×10^{5}	1.85×10^{5}	1.49×10^{5}	1.15×10^{6}	3.23×10^{5}
E_1''	2.26×10^{8}	3.86×10^{11}	5.66×10^{8}	6.94×10^{8}	1.28×10^{13}	1.41×10^{11}
E_2''	6.09×10^{7}	2.53×10^{11}	1.78×10^{8}	1.95×10^{9}	7.48×10^{12}	3.36×10^{10}
A_1'	2.68×10^{4}	1.63×10^{5}	1.25×10^{4}	4.01×10^{4}	4.76×10^{4}	1.37×10^{4}
E_3''	4.80×10^{8}	2.18×10^{8}	1.13×10^{8}	4.98×10^{8}	1.07×10^{11}	1.70×10^{11}
E_4''	1.09×10^{9}	7.13×10^{8}	1.24×10^{8}	2.52×10^{9}	2.36×10^{11}	6.28×10^{10}
E_1'	1.26×10^{7}	1.03×10^{7}	2.04×10^{7}	1.10×10^{7}	4.57×10^{7}	7.35×10^{7}
E_2'	5.38×10^{4}	7.05×10^{4}	1.76×10^{5}	1.70×10^{5}	1.89×10^{5}	3.32×10^{5}
A''	1.12×10^{11}	4.97×10^{7}	5.70×10^{9}	4.17×10^{10}	6.65×10^{11}	8.57×10^{10}
A_2'	3.52×10^{5}	4.84×10^{5}	2.01×10^{5}	2.13×10^{6}	2.36×10^{6}	8.62×10^{5}

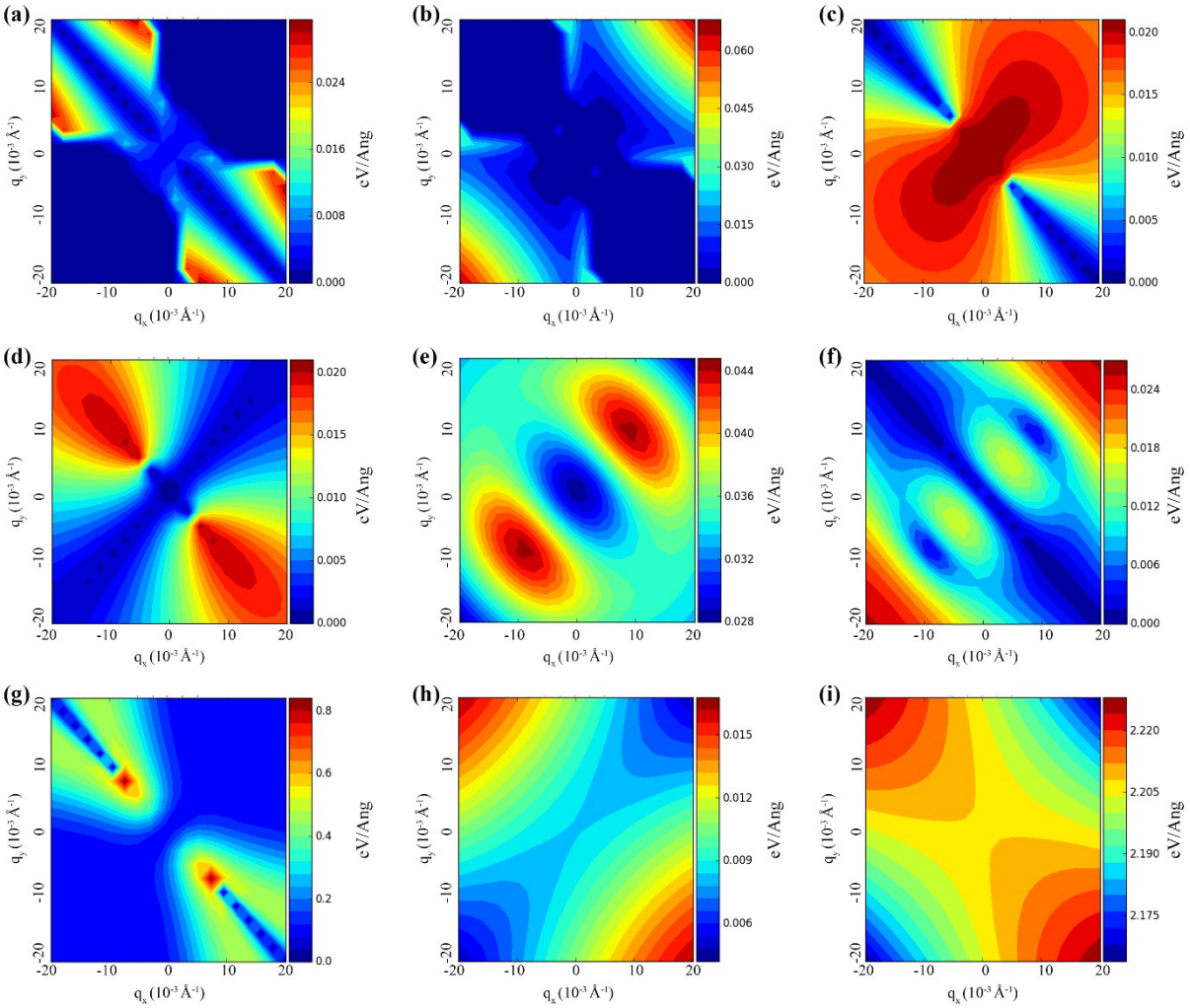

Fig. S1 The electron-phonon interaction matrix elements $|M^{\lambda}_{\mathbf{kq}}|$ of (a) ZA, (b) TA, (c) E_1'', (d) E_2'', (e) E_3'', (f) E_4'', (g) E_1', (h) A'', and (i) A_2' phonon modes in InS monolayer

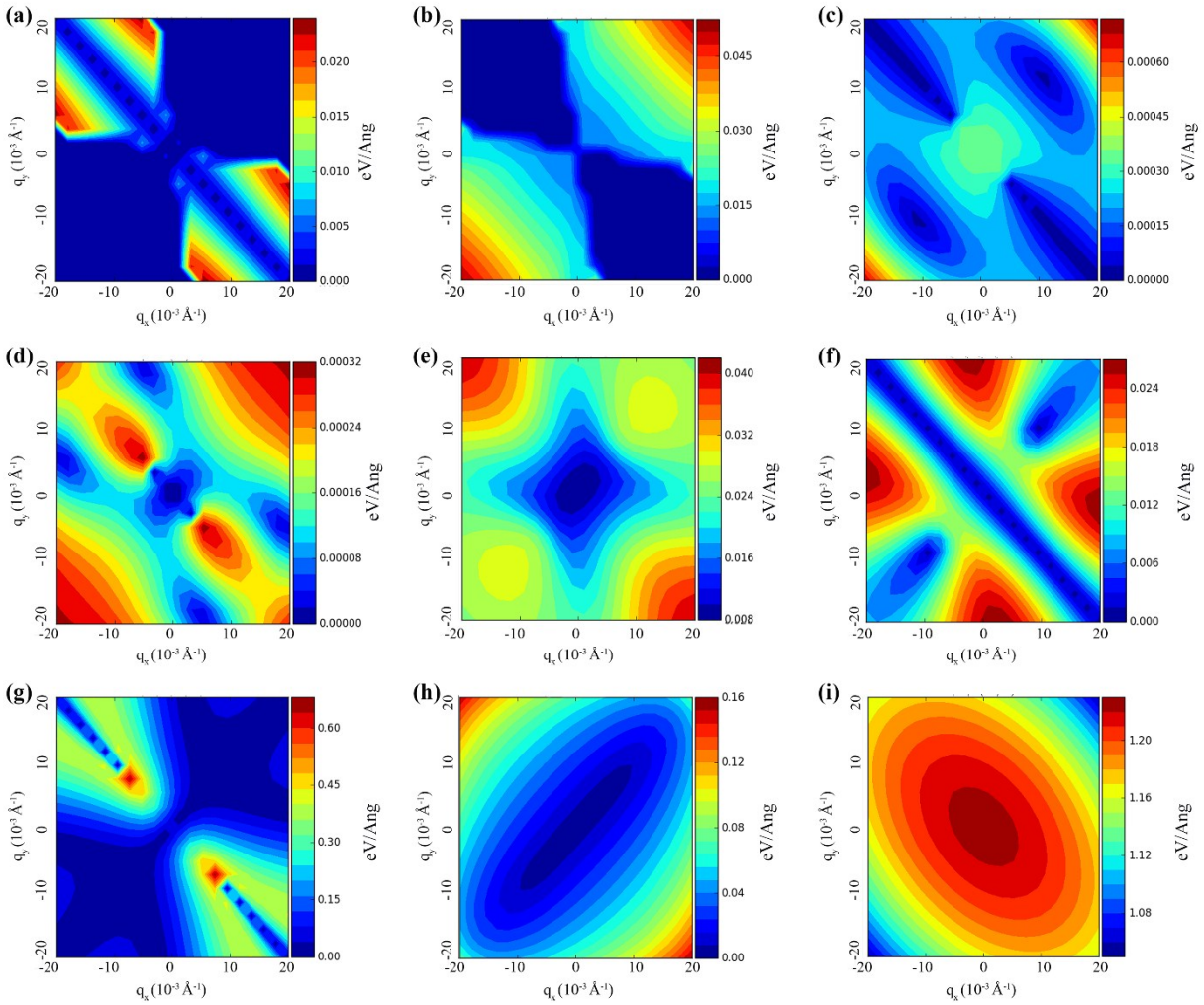

Fig. S2 The electron-phonon interaction matrix elements $|M^{\lambda}_{\mathbf{kq}}|$ of (a) ZA, (b) TA, (c) E_1", (d) E_2", (e) E_3", (f) E_4", (g) E_1', (h) A", and (i) A_2' phonon modes in InSe monolayer

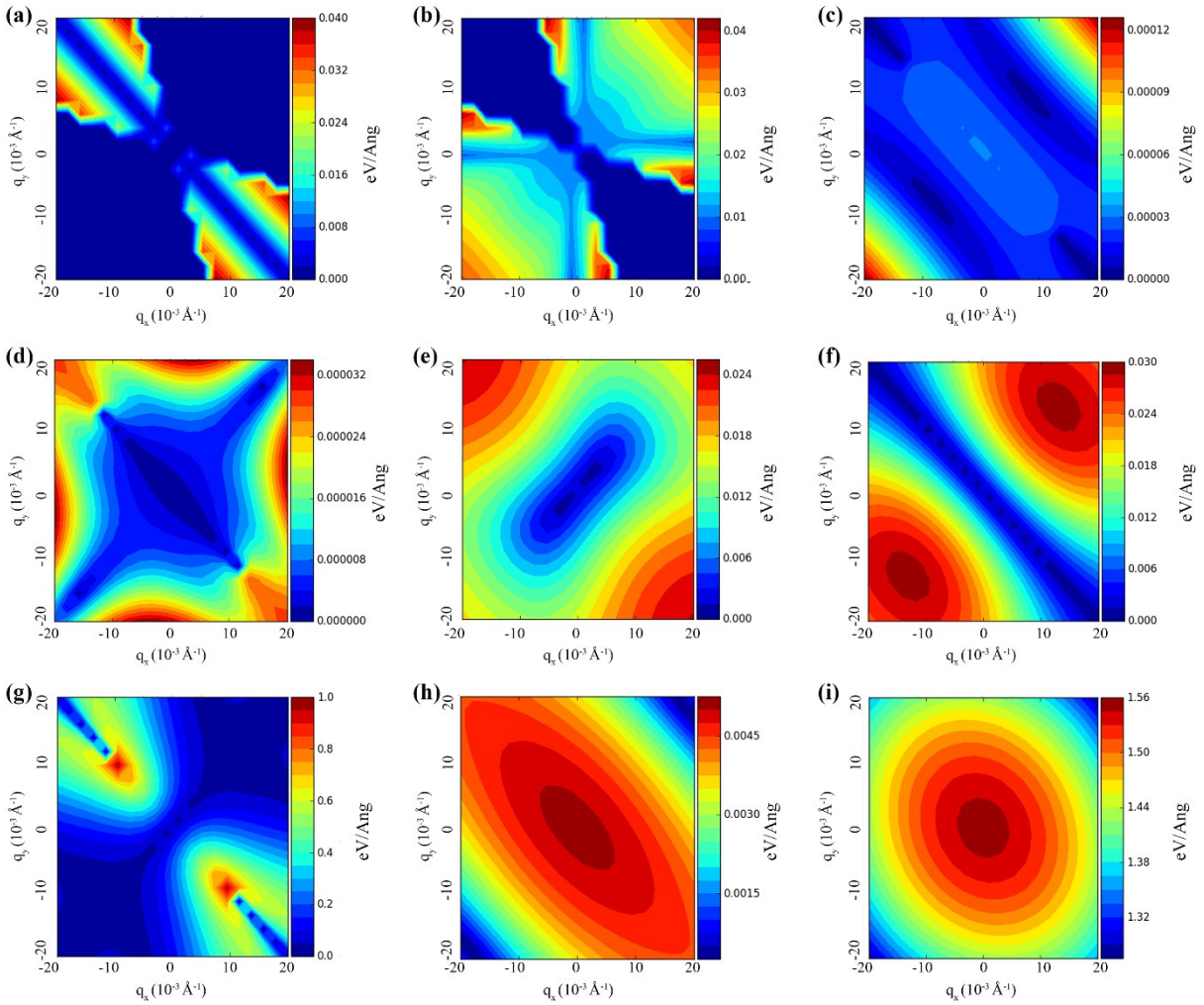

Fig. S3 The electron-phonon interaction matrix elements $|M_{\mathbf{kq}}^{\lambda}|$ of (a) ZA, (b) TA, (c) E_1'', (d) E_2'', (e) E_3'', (f) E_4'', (g) E_1', (h) A'', and (i) A_2' phonon modes in InTe monolayer

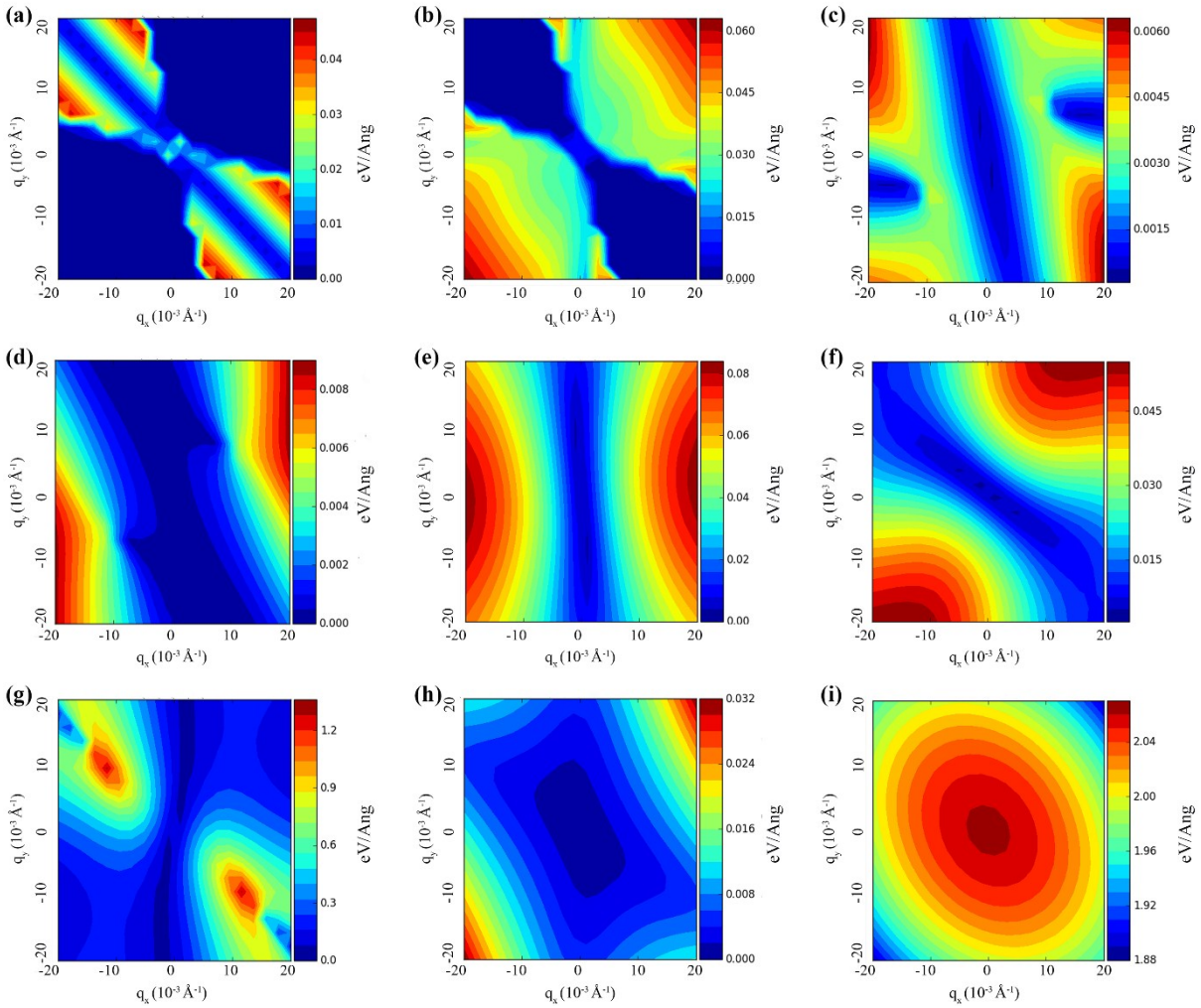

Fig. S4 The electron-phonon interaction matrix elements $|M_{\mathbf{kq}}^{\lambda}|$ of (a) ZA, (b) TA, (c) E_1'', (d) E_2'', (e) E_3'', (f) E_4'', (g) E_1', (h) A'', and (i) A_2' phonon modes in GaS monolayer

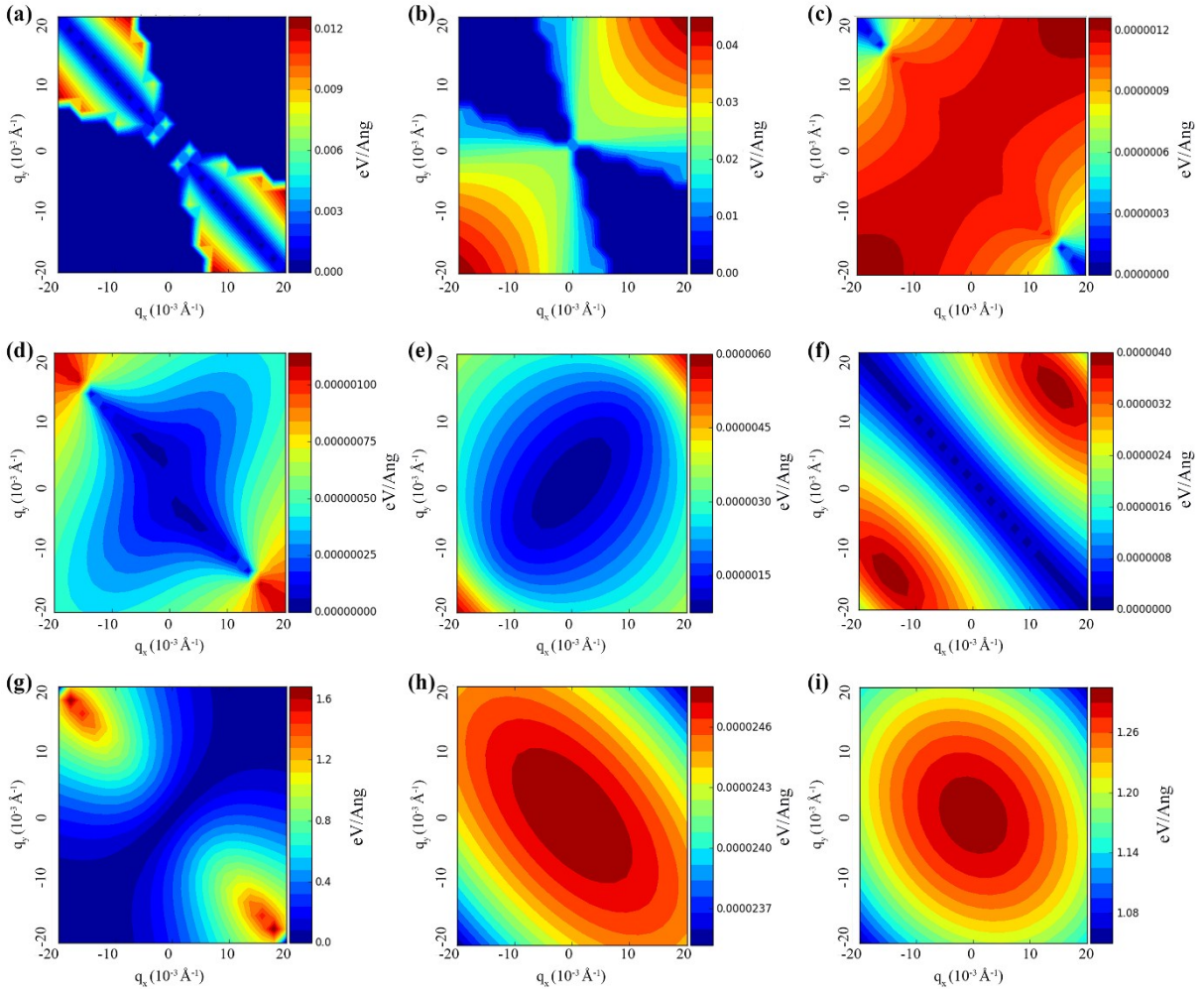

Fig. S5 The electron-phonon interaction matrix elements $|M^{\lambda}_{\mathbf{kq}}|$ of (a) ZA, (b) TA, (c) E_1'', (d) E_2'', (e) E_3'', (f) E_4'', (g) E_1', (h) A'', and (i) A_2' phonon modes in GaSe monolayer

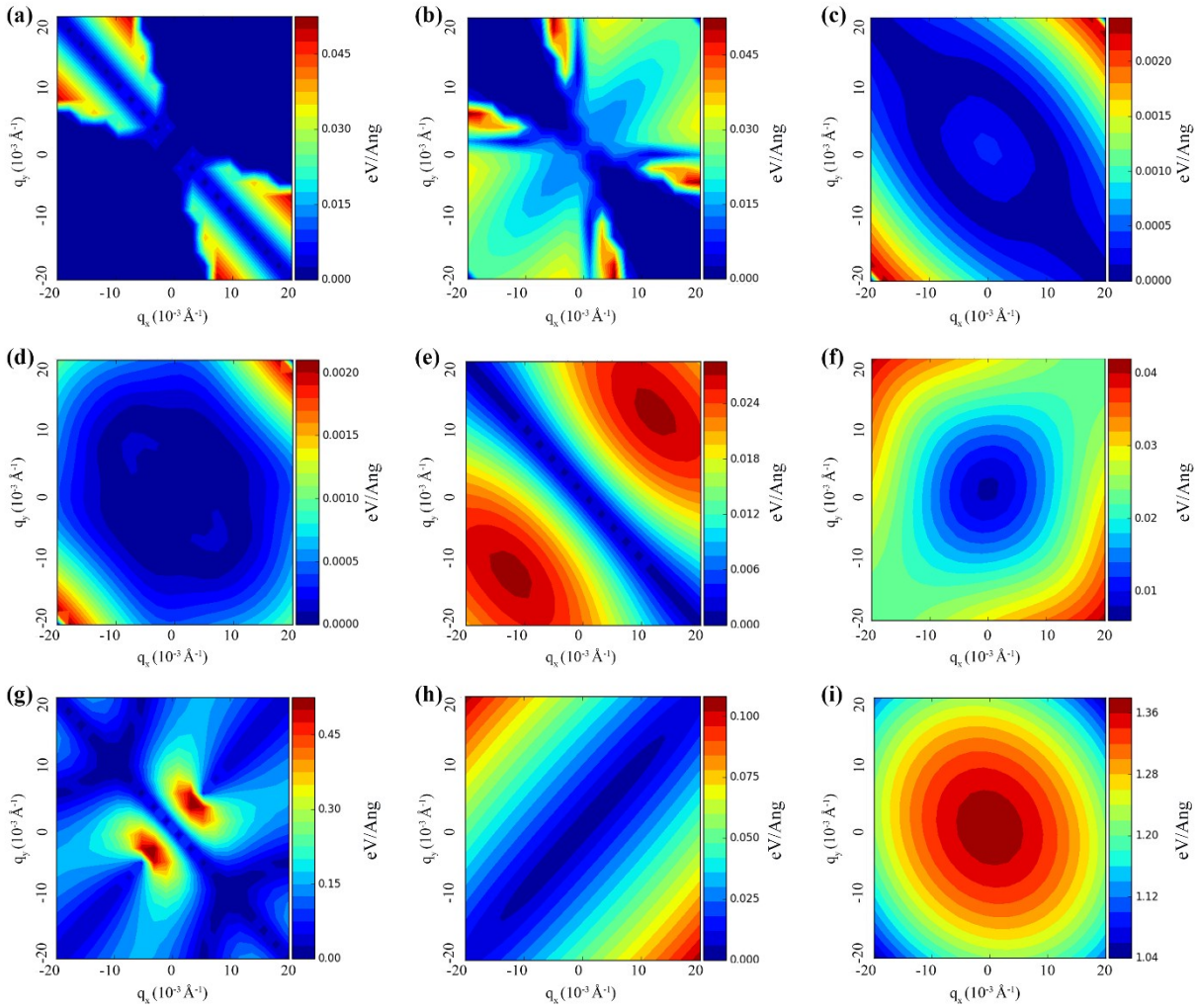

Fig. S6 The electron-phonon interaction matrix elements $|M_{\mathbf{kq}}^{\lambda}|$ of (a) ZA, (b) TA, (c) E_1'', (d) E_2'', (e) E_3'', (f) E_4'', (g) E_1', (h) A'', and (i) A_2' phonon modes in GaTe monolayer

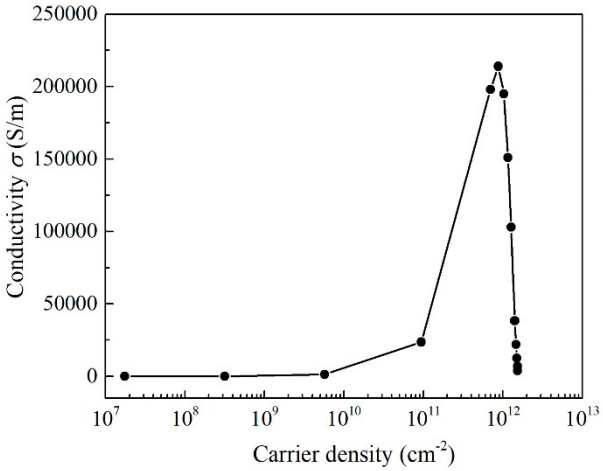

Fig S7. The calculated conductivity of GaSe monolayer versus to carrier concentration at 200 K.